Transactions of the Korean Nuclear Society Virtual Autumn Meeting
October 21-22, 2021

Zinc Addition Effects on Corrosion Behavior of Duplex Fe-Cr-Al alloy.

Su Hyun Park[a], Chaewon Kim[a], Hyeon Bae Lee[a], Changheui Jang[a,*]
[a]*Korea Advanced Institute of Science and Technology, Daejeon, Korea*
[*]*Corresponding author: chjang@kaist.ac.kr*

1. Introduction

As the generation of hydrogen gas was found to be the main cause of the explosion during 2011 Fukushima accident, there have been many efforts to reduce hydrogen-related problems. A most certain way to improve these problems might be a change of fuel cladding material [1]. Zircaloy cladding has been used because this alloy shows reasonable performance at normal operation conditions and shows extremely low neutron absorption cross-section so less neutron penalty. However, Zircaloy cladding has severe corrosion problem and produce hydrogen during an accident. The proposed accident tolerant fuel (ATF) cladding material are Mo-Zr alloy, Fe-based alloy, and SiCf/SiC cladding or cladding coatings [1].

ATF cladding materials are required to have high resistance to oxidation and corrosion. Autor's group has developed model alumina-forming duplex stainless steel (ADSS) as a candidate of ATF claddings material [2]. Fe-based material like ADSS shows a high neutron absorption cross-section leading to neutron penalty, so cladding thickness should be minimized. Meanwhile, Zn addition was adapted to reduce radiation dose in primary coolant conditions, and the number of plants applying zinc addition has been increasing since it was reported that they improve corrosion behavior of stainless steels and Ni-based alloy in PWR conditions [3, 4]. Since corrosion of ATF cladding material candidate ADSS is emphasized, zinc addition effects on corrosion behavior of this alloy are evaluated with normal PWR operational conditions by observing oxide film.

2. Experimental

2.1 Test material

The ADSS #B51 is used in this study. The chemical composition of this alloy is presented in table 1. ADSS #B51 has 3 different phases of austenite, ferrite, B2-NiAl phase. [2]. The surface image of ADSS #B51 before the immersion test is presented in Fig. 1. Surface observations are performed after 1 μm polishing. B2-NiAl phases are spread out with fine shape in austenite and a relatively large circular shape in the ferrite region. Test materials are machined as coupon specimens (15 mm × 16 mm × 1 mm with 1 mm diameter of a hole). Specimens are ground with silicon papers up to 600 # grit to represent industrial grade. Six specimens are used in PWR immersion and 3 specimens are used in the Zn-added PWR immersion test.

2.2 Immersion test condition

The immersion tests of coupon specimens are performed in simulated PWR primary water condition with and without 30 ppb zinc addition for 600 h. Test system is consisted of a once-through loop as shown in Fig. 2. The temperature and pressure are maintained at 325℃ and 15 MPa during the entire test period. The test solution is prepared by mixing distilled water with 1200 ppm of boric acid (H_3BO_3) and 2.2 ppm lithium hydroxide (LiOH) and for Zn-PWR cases 30ppb of zinc acetate ($C_4H_6O_4Zn$), which shows the conductivity of 22-25 μS/cm. The mixed solution was fed to the 1st tank which is purged with argon gas to reduce dissolved oxygen (DO) level and the 2nd tank which are purged with hydrogen gas to reach target dissolved hydrogen (DH, 25 cc/kg) and dissolved oxygen (DO, less than 5 ppb) level. The 2nd tank is pressurized at about 90 kPa to achieve the target DH level. The flow rate of the solution is 2.2 L/h which means that the solution in the autoclave is refreshed every 20 min. The test conditions are summarized in table 2, and inlet and outlet solutions are monitored and kept target value during the test.

2.3 Oxide film characterization

Weight of coupon specimen are measured before and after PWR (without and with Zn) immersion test with microbalance which has a resolution of 0.001 mg. Weight change during the test is expressed as mg/dm^2 by dividing with the surface area include the hole. The surface of specimens is observed by using field emission scanning electron microscopy (FE-SEM) equipped with energy dispersive spectroscopy (EDS). Cross-sectional analysis of oxide layer is conducted by transmission electron microscopy (TEM) with TEM specimen prepared by focused ion beam (FIB) method.

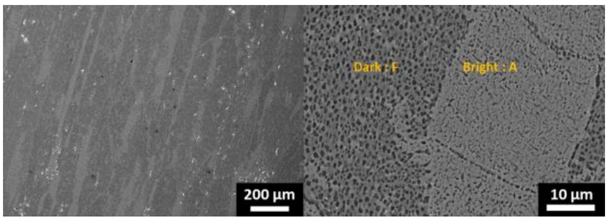

Figure 1. Surface area image of ADSS #B51 after 1μm polished before immersion test.

Table 1. Chemical composition of the alloy used in this study.

Composition [wt.%]	Fe	Ni	Cr	Al	Nb	Mn	C	Si
ADSS #B51	Bal.	18.98	16.13	5.90	0.51	1.01	0.12	0.31

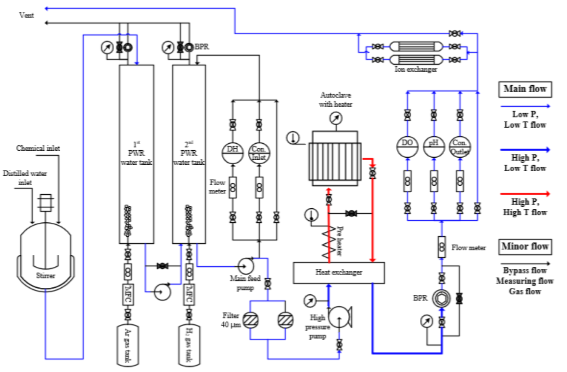

Figure 2. The schematic of simulated PWR loop used in this study

Table 2. Test condition used in this study.

Simulated PWR environment		without Zn	with Zn
Temperature		325℃	
Pressure		15 MPa	
Water chemistry	Dissolved hydrogen	25 cc/kg	
	Dissolved Oxygen	< 5 ppb	
	Conductivity	22-25 µS/cm	
	Zn concentration	0	30 ppb

Electrochemical analysis is conducted for evaluating the semiconductor characteristics of the oxide layer in this study. The coupon specimen is welded with copper wire and the whole area except the test area is insulated with transparent nail polish and non-acetic acid silicon. Electrochemical tests are conducted by a typical 3 electrode system composed with a saturated calomel electrode as a reference, a small platinum plate as a counter electrode, and a test specimen as a working electrode. Borated buffer solution (0.05 M H_3BO_3 + 0.075 M $Na_2B_4O_7$, pH 9.2) is used to conduct electrochemical impedance (EIS) and Mott-Schottky (M-S) analysis. EIS analyses are conducted at the open circuit potential (OCP) state in buffer solution. The AC amplitude of 10 mV and frequency range of 1 kHz to 0.01 Hz are used Point defect density is calculated with M-S analysis conducted with potential range -0.6 V (SCE) to +0.6 V (SCE) with a scanning rate of 10 mV.

3. Results

3.1 Weight change

Weight changes are presented in Table 3. Weight gain is reduced by about 30% in the Zn-added PWR environment than typical PWR environment. These results can be interpreted as less corrosion in the Zn-added environment.

3.2 Surface observation

Surface images are observed after 600 h immersion test in PWR without and with Zn and the results are presented in Fig. 3. The large B2-NiAl phase in the ferrite region creates relatively large oxide particles than ferrite without B2-NiAl and austenite regions. This result might come from different Cr contents (B2-NiAl phase include 3 wt.% of Cr and 16.8, 26.5 wt.% for austenite and ferrite, respectively). Despite quite high Cr contents in the ferrite region, oxide particles show similar size with particles on other phases. The inner oxide layer on the ferrite region is protective enough which is results from high Cr contents, but many metal ions are diffused out by a large B2-NiAl area that makes poor corrosion behavior even in the ferrite region [5]. The overall size of particles decreases with 30 ppb Zn addition, which might be expected from weight change data mentioned above.

Zinc is considered as stabilizing element of oxide with substituting Fe than forming stable oxide ZnFe2O4 and ZnCr2O4 [4]. Particle-free region are observed in ferrite region of PWR immersion specimen, however smaller size oxide particles are filled up the whole surface of ferrite, so number density of oxide particles are higher in Zn-added PWR than typical PWR environment. Although the maximum size of oxide particle is smaller in Zn added PWR condition, it is similar and the number density of oxide particles is higher in Zn PWR conditions. These results make the oxide stabilization effect of Zn on ADSS #B51 suspicious.

Table 1. Weight change after 600hr immersion test

Test environment	Weight gain [mg/dm^2]
PWR	2.95±0.33
Zn-PWR	2.14±0.30

3.3 Cross sectional observation

For a detailed understanding of Zn effects on the oxide layer of ADSS #B51, the chemical composition of the oxide layer should be analyzed by TEM. TEM analyses are on-going and results will be presented and discussed.

3.4 Electrochemical analysis

Electrochemical characteristics are also helpful to understand Zn effects on oxidation of ADSS #B51. A Nyquist plot which is the result of the EIS test is presented in Figure 4. The radius of the capacitance loop is usually considered an indicator of reaction resistance [4]. With Zn addition, the radius of the capacitance loop is smaller, or similar, than a typical PWR environment. This result makes Zn effects suspicious, as with the number density of oxide particles on the surface.

Electrochemical variable fitting process and Mott-Shottky (M-S) analysis are on-going to evaluate electrochemical properties of oxides. These results will be also prepared and presented.

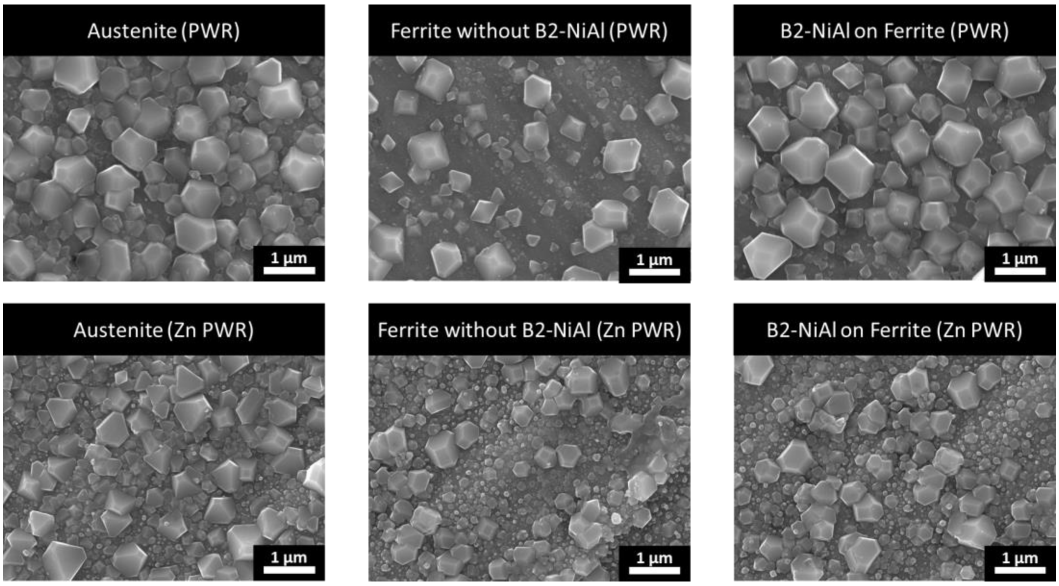

Figure 3. Surface image after 600hr immersion test in PWR environment without and with Zn.

4. Conclusions

Zn addition effects on developed alloy ADSS #B51 are evaluated by immersion test in simulated PWR loop for 600hr.

- The weight change in the Zn-added PWR immersion test is smaller than typical PWR conditions by about 30%.
- The overall size of oxide particles is smaller in the Zn-added PWR condition, but size differences are not significant.
- Although the oxide stabilization effect of Zn was expected, a higher number density of oxide particles was observed.
- The Nyquist plot which is one of the results of the EIS test shows slight reaction resistance decrease, or similar, with Zn addition that is opposite with expectation.
- A more detailed analysis (TEM, electrochemical analysis) about the Zn effect on ADSS #B51 will be conducted and presented.

REFERENCES

[1] H.-G. Kim, J.-H. Yang, W.-J. Kim, Y.-H. Koo, Development status of accident-tolerant fuel for light water reactors in Korea, Nuclear Engineering and Technology 48(1) (2016) 1-15.

[2] H. Kim, H. Jang, G.O. Subramanian, C. Kim, C. Jang, Development of alumina-forming duplex stainless steels as accident-tolerant fuel cladding materials for light water reactors, Journal of Nuclear Materials 507 (2018) 1-14.

[3] E. TR-1009568, Overview Report on Zinc Addition in Pressurized Water Reactors-2004, 2004.

[4] H.B. Lee, J. Chen, S. Meng, C. Jang, S.H. Park, Q. Xiao, H.J. Lee, K.-H. Na, Characterization of oxide layers formed on type 316 stainless steel exposed to the simulated PWR primary water environment with varying dissolved hydrogen and zinc concentrations, Journal of Nuclear Materials (2021) 153193.

[5] Q. Xiao, C. Jang, C. Kim, H. Kim, J. Chen, H.B. Lee, Corrosion behavior of stainless steels in simulated PWR primary water: The effect of composition and matrix phases, Corrosion Science 177 (2020) 108991.

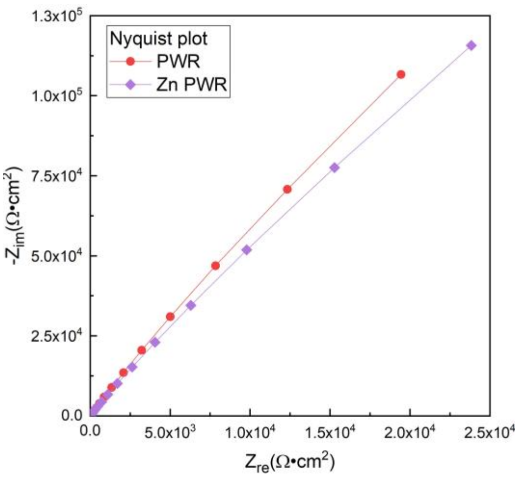

Figure 4. Nyquist plot of oxide film on ADSS #B51